Non-Darcy Newtonian Liquid Flow with Internal Heat Generation using Boundary Conditions of the Third Kind of Fully Developed Mixed Convection in a Vertical Channel

Nurul Asyiqin Mat Yaman[1], Nur Asiah Mohd Makhatar[1,*], Mohd Rijal Ilias[1], Abdul Rahman Mohd Kasim[2], Nurul Farahain Mohammad[3]

1   Faculty of Computer and Mathematical Sciences, Universiti Teknologi MARA Shah Alam, 40450 Shah Alam, Selangor, Malaysia
2   Centre for Mathematical Sciences, College of Computing & Applied Sciences, Universiti Malaysia Pahang, Lebuhraya Tun Razak, Gambang 26300, Pahang, Malaysia
3   Department of Computational and Theoretical Sciences, Kulliyyah of Science, International Islamic University Malaysia, Bandar Indera Mahkota, 25200 Kuantan, Pahang, Malaysia

ARTICLE INFO	ABSTRACT
	An analysis of the impact of internal heat generation and other heat parameters on the temperature, velocity and rate of heat transfer of the liquid moving upward in a channel is studied. A fully developed non-Darcy flow using boundary conditions of the third kind with internal heat generation in a vertical channel is selected as the mathematical model. By utilising the similarity transformation, the governing equations are reduced to non-linear ordinary differential equations (ODEs). The converted ODEs are numerically solved and analysed using the fourth-order Runge-Kutta (RK4) method, incorporating a shooting technique with Newton's method. The generated numerical algorithms are programmed in MATLAB for velocity, temperature and the local Nusselt number analysis. The numerical results of the flow and temperature variables are presented graphically. The impact of the parameters on the Nusselt number is also graphed to determine which of the three types of boundary conditions is the best for allowing heat transmission. The severity of flow reversal is increased under the Robin and Dirichlet conditions by enhancing the Darcy and Forchheimer numbers while decreasing the Brinkman and internal heat generation values. The temperature profiles improved with the increase in Brinkman numbers. Both Nusselt numbers remained constant for the Neumann boundary condition for all parameters except internal heat generation and local heat exponent. The Robin boundary condition is found to be the best facilitates heat transmission, since it delivers more pleasing and realistic results than the Dirichlet and Neumann conditions.

1. Introduction

The present rate of technology innovation with more sophisticated technologies has significantly affected the lifestyle of individuals. Heat transfer is a ubiquitous feature in manufacturing when

producing goods demands steady and suitable heat to develop more innovative technologies. In the industry sectors, heat transfer via vertical tubes is commonly used in cooling devices for electronics, nuclear waste disposal and many more applications. There have been a few kinds of research on wall-bounded mixed convection through vertical channels. The earliest analyses of fully developed mixed heat convection through vertical channels can be found in the work of Tao [18] and Agrawal [1]. Since then, many academics have received considerable attention to the effects of mixed convection flow in a vertical channel. It has been proven as a new efficient heat transmission mechanism for many applications. Prasad *et al.,* [14] reviewed the influence of viscous dissipation on the fully developed combination of mixed convection and radiation effect in a vertical channel. Kalyan *et al.,* [8] have analyzed the impact of a material characteristic on fully developed mixed convective micro-polar fluid flow in a vertical channel. Furthermore, chemical reaction improved flow reversal and allowed flow reversing for symmetrical wall temperatures [16]. These kinds of research have broadened the significant variables affecting heat transmission.

Boundary conditions are divided into three categories: Dirichlet, Neumann, and Robin boundary conditions. Analysis by Kumar *et al.,* [10] revealed that for equal Biot numbers, flow reversal was shown for asymmetric wall heating but not for unequal Biot numbers. Pajera [13] concluded that the nature of the studied thermal loading causes the construction of Robin boundary conditions, which can be interpreted as a mixture of Dirichlet and Neumann boundary conditions. Many authors may find detailed discussions on the boundary conditions in review articles [9, 21].

Internal heat generation is the unique strategy for enhancing the heat transfer rate that has generated more heat. Many studies, like Tritton and Zarraga [20], explained that heat is produced throughout the fluid and in areas with zero velocity. It was further said by Ferdows *et al.,* [6] that momentum diffusion results in making internal heat. They also observed that internal heat generation caused more flow in terms of temperature distribution. The velocity profiles are examined, but it is found that none of them significantly affects the results. Under the effect of internal heat generation, Saba *et al.,* [15] discovered when the temperature rises, the heat generation parameter is thought to increase. Norhaliza and Rozaini [25], Travis and Olson [19] and Mealey and Merkin [11] have published studies on heat transfer in the presence of internal heat generation.

There must be precautions to prevent dangerous events when choosing improper liquid features. Earlier investigations on the flow of fluids through porous media were confined to Newtonian fluids [17]. Because of its importance in industrial usage, the flow of non-Newtonian fluids through porous media has gotten much attention since then [22]. According to the studies by Broniarz-Press and Pralat [4], the thermal conductivity of both Newtonian and non-Newtonian liquid systems decreased as the liquid's viscosity increased. However, Chinyoka [5] demonstrates that Newtonian fluids are far more prone to thermal runaway processes when compared to viscoelastic fluids. Besides, A lot of scholars have also looked at various issues concerning non-Newtonian and Newtonian liquids [3, 7, 24].

The present research explores non-Darcy flow using the boundary conditions of the third kind with internal heat generation of mixed convection through a vertical channel. In this research, internal heat generation for heat transmission through the vertical channel is extended to the work of Mohd Makhatar *et al.,* [12]. Except for the internal heat generation, the research already provides this study's flow characteristics. Therefore, this research introduced internal heat generation into the analogous instance of heat transfer.

2. Methodology
2.1 Mathematical Formulation

In this study, mixed convection non-Darcy flow with internal heat generation is investigated. Consider a two-dimensional Newtonian fluid flowing steadily in $L-$ width parallel plate vertical channel. Figure 1 shows X-axis is located in the axial plane of the channel, and travels in the opposite direction of the gravitational force, $\boldsymbol{g}$. The $Y-$ axis is perpendicular to the channel walls, and the walls at $Y = -L/2$ and $Y = -L/2$ are isothermal at given temperature T_C and T_H respectively. The flow has a uniform upward vertical velocity, U_0 at the channel entrance.
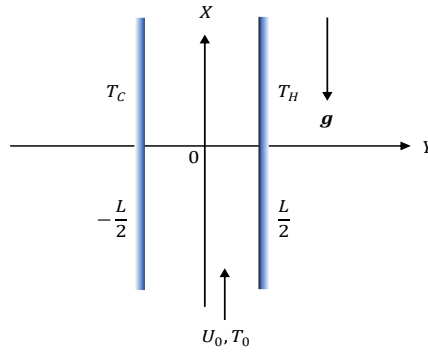
Fig. 1. Graphical Form.

Natural convective flow is governed by coupled partial differential equations, which are quite complicated. As customary, the Boussinesq-Oberbeck approximation and the equation of state:

$$\rho = \rho_0[1 - \beta(T - T_0)] \tag{1}$$

are adopted where ρ_0 and T_0 are the reference density and temperature respectively. β is the thermal expansion coefficient.

It is assumed that the only nonzero component of the velocity field U is the X-component $U(Y)$ so that the flow is a fully developed flow. Thus, the following relations apply:

$$V = 0, \quad \frac{\partial U}{\partial X} = 0 \tag{2}$$

Since $\nabla \cdot \boldsymbol{U} = 0$, so that U depends only on Y. U and V are the velocity components along vertical and horizontal respectively. The momentum balance equations along X and Y directions are:

$$\beta \boldsymbol{g}(T - T_0) = \frac{1}{\rho_0}\frac{\partial P}{\partial X} - v\frac{d^2 U}{dY^2} + \frac{v}{K}U + \frac{C_F}{\sqrt{K}}U^2 \tag{3}$$

$$\frac{\partial P}{\partial Y} = 0 \tag{4}$$

where $v = \mu/\rho_0$ is the kinematic viscosity, p is the fluid pressure, $P = p + \rho_{0gX}$ is the difference between the pressure and the hydrostatic pressure, T is the local temperature, K is the permeability of porous medium and C_F is the inertial coefficient.

Differentiating Eq. (3) with respect to X and then separately with respect to Y, we obtain:

$$\frac{\partial T}{\partial X} = \frac{1}{\beta g \rho_0} \frac{d^2 P}{dX^2} \tag{5}$$

$$\frac{\partial T}{\partial Y} = -\frac{v}{\beta g} \frac{d^3 U}{dY^3} + \frac{v}{\beta g K} \frac{\partial U}{\partial Y} + \frac{2C_F}{\beta g \sqrt{K}} U \frac{\partial U}{\partial Y} \tag{6}$$

$$\frac{\partial^2 T}{\partial Y^2} = -\frac{v}{\beta g} \frac{d^4 U}{dY^4} + \frac{v}{\beta g K} \frac{\partial^2 U}{\partial Y^2} + \frac{2C_F}{\beta g \sqrt{K}} \left[U \frac{\partial^2 U}{\partial Y^2} + \left(\frac{\partial U}{\partial Y}\right)^2 \right] \tag{7}$$

Since Eq. (5) ensures that $\frac{\partial T}{\partial X}$ does not depend on Y, it is concluded that $\frac{\partial T}{\partial X}$ is zero everywhere. Therefore, the temperature T depends only on Y. Thus, we may write:

$$\frac{\partial P}{\partial X} = A ; \qquad \text{where } A \text{ is constant.} \tag{8}$$

The boundary conditions on U are taken as follows:

$$U\left(-\frac{L}{2}\right) = U\left(\frac{L}{2}\right) = 0 \tag{9}$$

The boundary conditions on the temperature field are assumed to be the following:

$$-k \frac{\partial T}{\partial Y}\Big|_{Y=-\frac{L}{2}} = h_1 \left[T_C - T\left(X, -\frac{L}{2}\right)\right] ; \qquad -k \frac{\partial T}{\partial Y}\Big|_{Y=\frac{L}{2}} = h_2 \left[T\left(X, \frac{L}{2}\right) - T_H\right] \tag{10}$$

where h_1 and h_2 are constants, k is the thermal conductivity, T_C and T_H are the temperature fluid at cool wall and at hot wall respectively. Using Eq. (6), Eq. (10) rewritten as:

$$\frac{d^3 U}{dY^3}\Big|_{Y=-\frac{L}{2}} = \frac{\beta g h_1}{kv} \left[T_C - T\left(X, -\frac{L}{2}\right)\right] ; \qquad \frac{d^3 U}{dY^3}\Big|_{Y=\frac{L}{2}} = \frac{\beta g h_2}{kv} \left[T\left(X, \frac{L}{2}\right) - T_H\right] \tag{11}$$

Eq. (11) implies that $\partial T/\partial X$ is zero both at $Y = -L/2$ and at $Y = L/2$. The conservation of energy equation is modified for the presence of internal heat generation:

$$k \frac{d^2 T}{dY^2} = -\mu \left(\frac{dU}{dY}\right)^2 - g \rho_0 c_p (T - T_0)^\lambda \tag{12}$$

where λ is local heating exponent.

$$U_0 = -\frac{AD^2}{48\mu}, \quad T_0 = \frac{T_C + T_H}{2} + S \left(\frac{1}{Bi_C} - \frac{1}{Bi_H}\right)(T_H - T_C) \tag{13}$$

was given, where the Biot number at cool wall, Bi_C and at hot wall, Bi_H are define as:

$$Bi_C = \frac{h_1 D}{k}, \quad Bi_H = \frac{h_2 D}{k} ; \qquad \text{where } D = 2L \text{ is the hydraulic diameter} \tag{14}$$

The non-Dimensionless form of the Nusselt number can be defined at each boundary as follows:

$$Nu_C = \frac{D}{R_T \left[T\left(\frac{L}{2}\right) - T\left(-\frac{L}{2}\right)\right] + (1 - R_T)\Delta T} \frac{dT}{dY}\Big|_{Y=-\frac{L}{2}}, \quad Nu_H = \frac{D}{R_T \left[T\left(\frac{L}{2}\right) - T\left(-\frac{L}{2}\right)\right] + (1 - R_T)\Delta T} \frac{dT}{dY}\Big|_{Y=\frac{L}{2}} \tag{15}$$

Eqs. (7), (9), (10) and (12) can be written in a dimensionless form by employing the following dimensionless parameters:

$$u = \frac{U}{U_0}, \qquad \theta = \frac{T-T_0}{\Delta T}, \quad y = \frac{Y}{D}, \qquad Gr = \frac{g\beta\Delta T D^3}{v^2}, \quad Br = \frac{\mu(U_0)^2}{k\Delta T}, \quad \alpha = \frac{k}{\rho_0 C_p},$$

$$Pr = \frac{v}{\alpha}, \qquad GR = \frac{Gr}{Re}, \quad R_T = \frac{T_H - T_C}{\Delta T}, \qquad Da = \frac{D}{\sqrt{K}}, \qquad F = ReC_F Da, \quad Re = \frac{U_0 D}{v},$$

$$S = \frac{Bi_C Bi_H}{Bi_C Bi_H + 2Bi_C + 2Bi_H}, \qquad G = \frac{g D^2 (\Delta T)^{\lambda-1}}{\alpha} \quad \text{in which } \Delta T = T_H - T_C. \tag{16}$$

where u is the dimensionless velocity along X- direction, θ is the dimensionless temperature, y is the axial coordinate, Gr is the Grashof number, Br is the Brinkman number, Pr is the Prandtl number, GR is the mixed convection parameter, G is the internal heat generation, R_T is the temperature difference ratio, F is the Forchheimer number, Re is Reynolds number, Da is Darcy number, S is a dimensionless parameter, α is the thermal diffusivity of the fluid, C_p is the specific heat at constant pressure, λ is the local heating exponent and $\Delta T = T_H - T_C$.

The non-dimensional governing equations are:

$$GR \frac{d^2\theta}{dy^2} = -\frac{d^4 u}{dy^4} + Da^2 \frac{d^2 u}{dy^2} + 2F \left[u \frac{d^2 u}{dy^2} + \left(\frac{du}{dy}\right)^2 \right] \tag{17}$$

$$\frac{d^2\theta}{dy^2} = -Br \left(\frac{du}{dy}\right)^2 - G\theta^\lambda \tag{18}$$

subject to the boundary conditions

$$u\left(-\frac{1}{4}\right) = u\left(\frac{1}{4}\right) = 0 \tag{19}$$

$$\frac{d\theta}{dy}\Big|_{y=-\frac{1}{4}} = Bi_C \left[\theta\left(-\frac{1}{4}\right) + \frac{R_T S}{2}\left(1 + \frac{4}{Bi_C}\right) \right] \tag{20}$$

$$\frac{d\theta}{dy}\Big|_{y=\frac{1}{4}} = Bi_H \left[-\theta\left(\frac{1}{4}\right) + \frac{R_T S}{2}\left(1 + \frac{4}{Bi_H}\right) \right] \tag{21}$$

Dimensionless equations for Nusselt numbers which derived at the left and right vertical channels are as follows:

$$Nu_C = \frac{1}{R_T\left[\theta\left(\frac{1}{4}\right)-\theta\left(-\frac{1}{4}\right)\right]+(1-R_T)} \frac{d\theta}{dy}\Big|_{y=-\frac{1}{4}}, \qquad Nu_H = \frac{1}{R_T\left[\theta\left(\frac{1}{4}\right)-\theta\left(-\frac{1}{4}\right)\right]+(1-R_T)} \frac{d\theta}{dy}\Big|_{y=\frac{1}{4}} \tag{22}$$

According to Zanchini [23], the dimensionless equations for the velocity field boundary condition are:

$$\frac{d^2 u}{dy^2}\Big|_{y=-\frac{1}{4}} - \frac{1}{Bi_C}\frac{d^3 u}{dy^3}\Big|_{y=-\frac{1}{4}} = -48 + \frac{R_T GR}{2} S\left(4 + \frac{1}{Bi_C}\right) \tag{23}$$

$$\frac{d^2 u}{dy^2}\Big|_{y=\frac{1}{4}} + \frac{1}{Bi_H}\frac{d^3 u}{dy^3}\Big|_{y=\frac{1}{4}} = -48 - \frac{R_T GR}{2} S\left(4 + \frac{1}{Bi_H}\right) \tag{24}$$

2.2 Numerical Method

The system of non-dimensional equations derived are numerically solved in this study. The boundary value problems for ODEs are solved using the fourth-order Runge-Kutta (RK4) method incorporating a shooting technique with Newton's method by treating the boundary value problems (BVPs) as the initial value problems (IVPs). After transforming to ordinary differential equations (ODEs) as described in the previous section, the shooting method is used to solve for the flow and temperature distributions for the governing equations. Newton algorithm is the most popular method and is simple and fast for locating roots of nonlinear systems of equations. Nevertheless, Newton algorithm requires a good initial guess to reach convergence to the solution. The method might never converge if the initial guess was very inaccurate. If the systems are linear, the narrative will be different. By introducing an auxiliary parameter, λ_a, it is possible to create a continuation that converts a nonlinear system to a linear one.

Figure 2 shows the flowchart for mixed convection in a vertical channel with internal heat generation. All of the solutions described here were written in MATLAB until the velocity, temperature and local Nusselt number profiles are displayed. The tolerance was set at 10^{-6}.
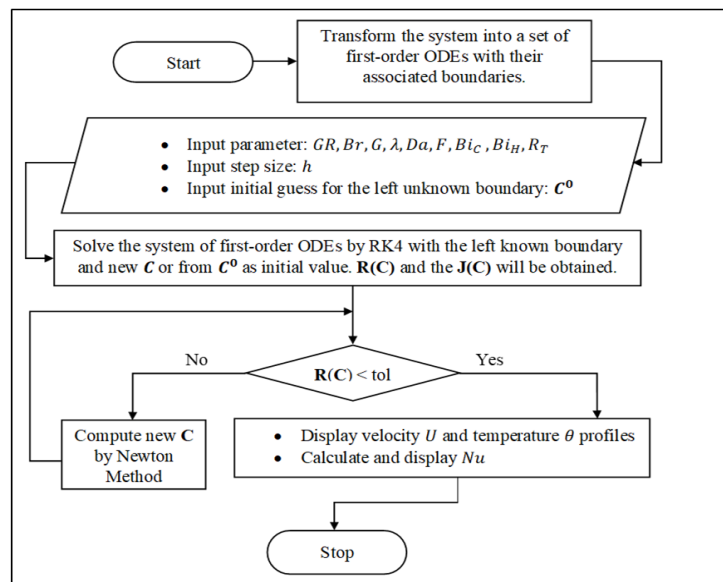
Fig. 2. Flowchart for Solution Procedure

2.3 Validation

The governing boundary layer equations are numerically solved using the shooting method. In some cases, validation is accomplished by comparing the current result to previously published output. Let $G = 0$, the result is compared with the results obtained by Barletta [2]. The effects of the relevant flow parameters on velocity and temperature are observed.

The existing model and its calculation results are acceptable because the output is seen to be similar to the reference findings acquired by Barletta (1998). Figures 3 and 4 indicate that the shooting outcomes are in good agreement with the available particular solutions. Thus, these intensive verification efforts demonstrated the validity of the current solution approach.

(a)   (b)
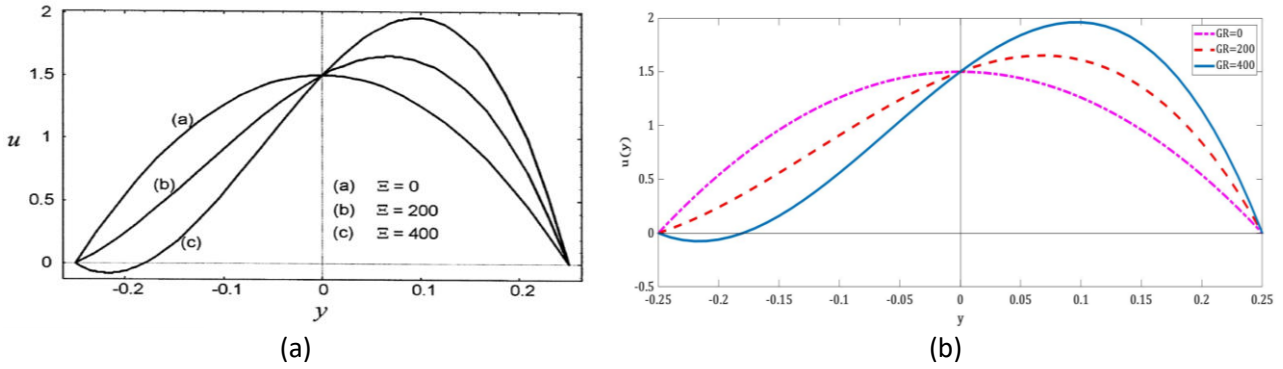
Fig. 3. Velocity profiles of (a) Barletta (1998) and (b) Present study for different GR with $Br = 0$

(a)   (b)
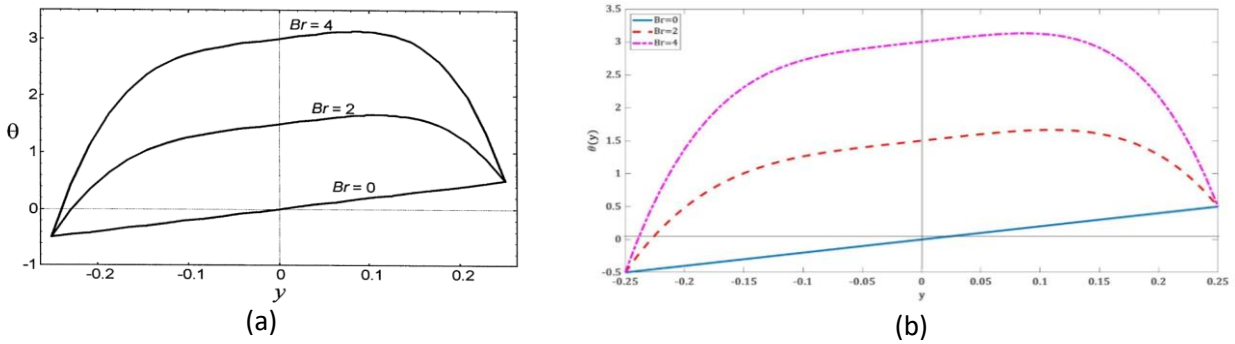
Fig. 4. Temperature profiles of (a) Barletta (1998) and (b) Present study for different Br with $GR = 0$

3. Results

The non-Darcy flow of fully developed mixed convection through a vertical channel in the presence of internal heat generation has been theoretically analysed. The solutions obtained for the dimensionless equations and the governing boundary are controlled by mixed convection parameter GR, Brinkman number Br, Darcy number Da, Forchheimer number F, internal heat generation G, heating exponent λ and Biot numbers at both walls, Bi_C and Bi_H. $R_T = 1$ is the fixed value for all cases representing the asymmetric fluid temperatures where $T_C < T_H$.

Figure 5 represents the velocity and the temperature profiles of the non-Darcy flow for several values of GR. In Figure 5a, the velocity distribution within the channel becomes less uniform as the magnitude of GR increases. The flow shrinks as it comes into contact with the colder wall, so that the velocity of the flow becomes lower as GR increases. This is because GR has revealed the effects of both natural and forced convection, with natural convection predominating in the flow and buoyant force regulating the flow. When the flow is upward, the density increases and the buoyancy force decreases as GR increases, leading to the reverse flow. The reflow phenomenon occurs with a high value of GR. Moving on to the temperature profile in Figure 5b, we can observe only minimal differences in the profiles for different GR values. This slight discrepancy is because of internal heat generation, which reduces the influence of GR values.

(a)

(b)
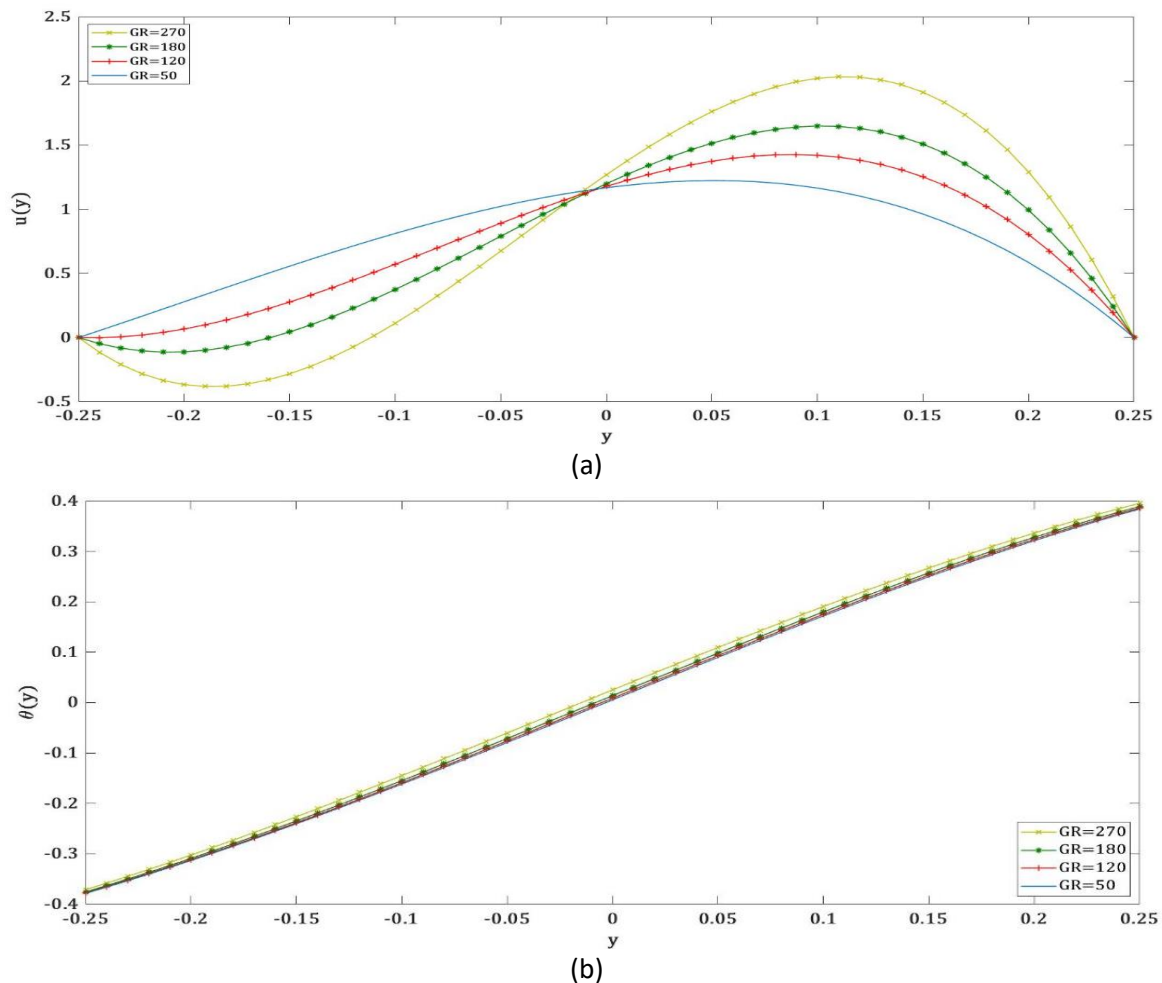
Fig. 5. Velocity and temperature profiles of non-Darcy flow for different values of GR with $Bi_C = Bi_H = 10, Br = 0.002, \ Da = 2, F = 3, G = 10$ and $\lambda = 1$

Figure 6 presents the effects of various values of Br on dimensionless velocity and temperature profiles. It is observed that the flow reversal becomes disappears as more Br is applied in Figure 6a. This is a natural consequence because increased Br enlarges the buoyancy effect because of more substantial dissipation, leading to higher fluid temperature. The higher temperature enhances the value of GR and therefore yields an increase in the fluid velocity. We can assume that the low value of Br enhances the reverse flow. Figure 6b depicts the temperature profiles, demonstrating that the temperature profile improved when Br was increased. The graphical results of dimensionless velocity and temperature distributions on different Da are shown in Figure 7. In Figure 7a, increasing the Da improves flow reversal while suppressing the maximum rate towards the hotter wall. This indicates that a higher Da reduces the speed at each place, which creates flow reversal near the cooler wall. Meanwhile, a lower Darcy number will provide greater velocity and the reversal flow will disappear more.

(a)

(b)
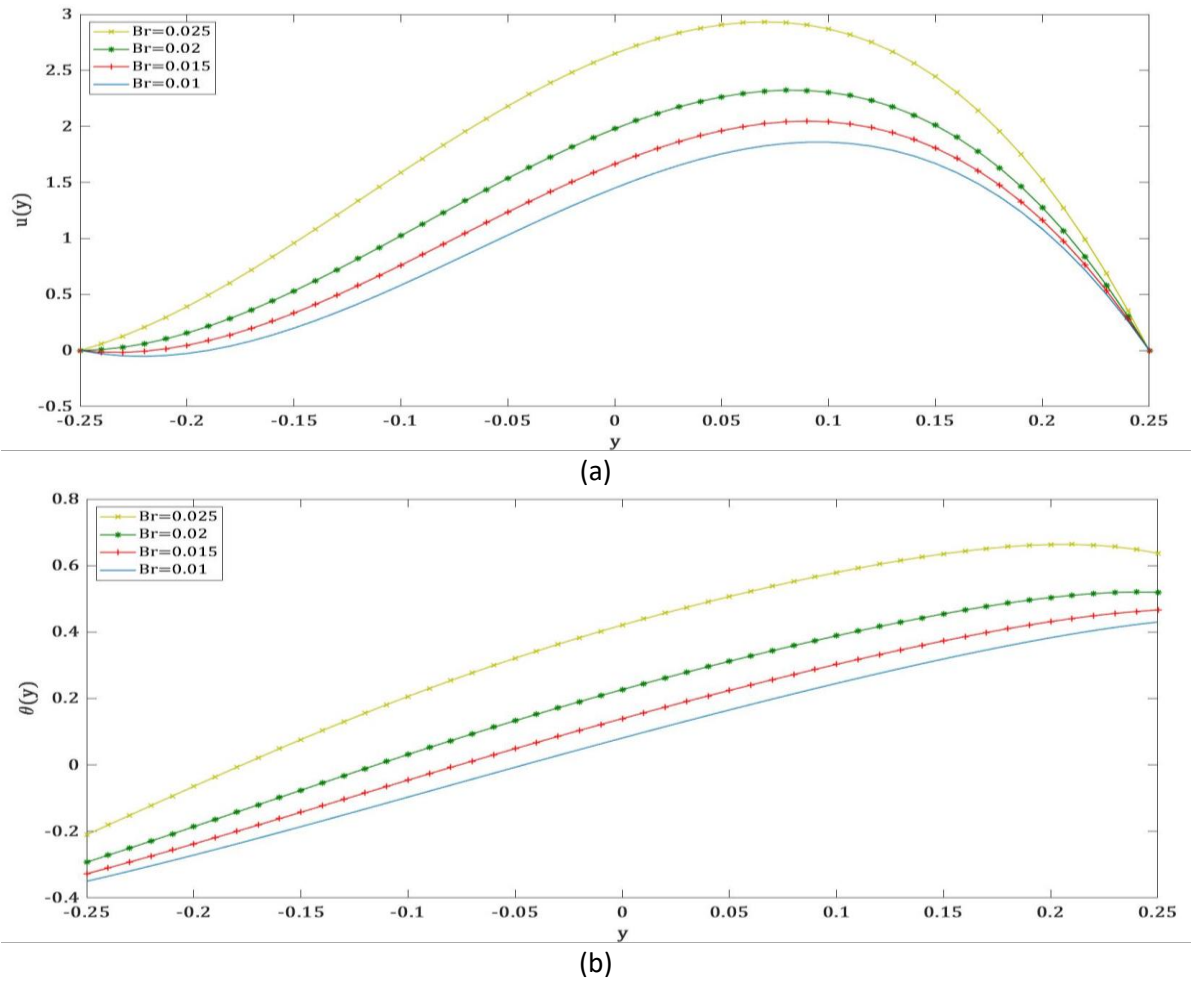
Fig. 6. Velocity and Temperature profiles of non-Darcy flow for different values of Br with $Bi_C = Bi_H = 10$, $GR = 180$, $Da = 2, F = 3, G = 10$ and $\lambda = 1$

(a)

(b)
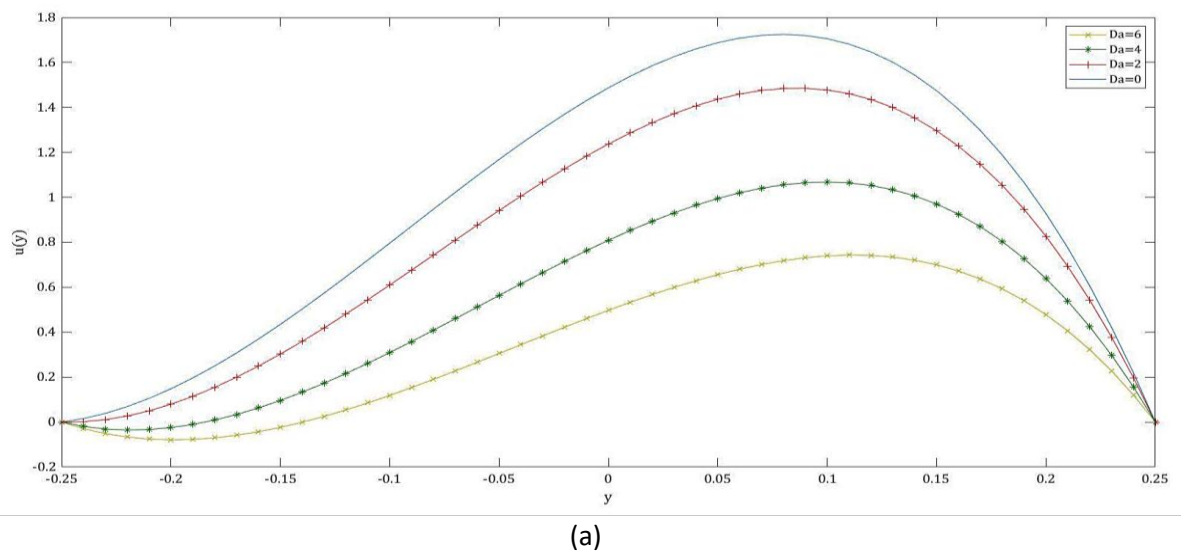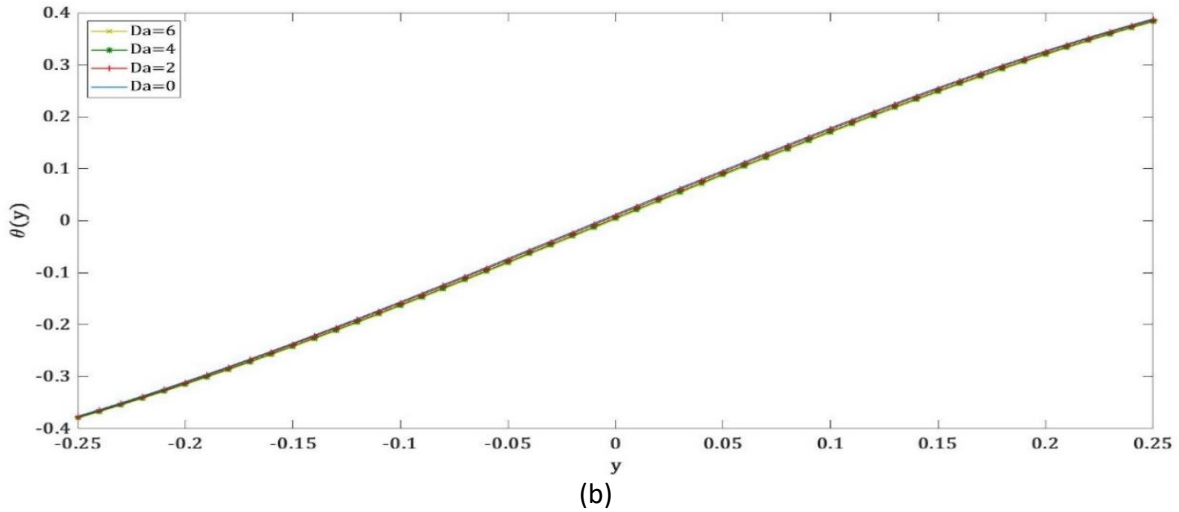
Fig. 7. Velocity and Temperature profiles of non-Darcy flow for different values of Da with $Bi_C = Bi_H = 10, \; GR = 120, \; Br = 0.002, F = 1, G = 10$ and $\lambda = 1$

Figure 8 illustrates the graph of the impact of Bi_C. The velocity profiles increase and skew to the right side of the wall with a smaller value of Bi_C in Figure 8a. However, the concavity of the velocity profile only appears when $Bi_C = 6$. This shift coincides with the inflection point in the middle of the channel, showing backflow near the cooler wall. Besides, the temperature profile will become more linear in Figure 8b with a smaller value of Bi_C. It is interesting to note that the thermal resistance of the channel decreases and convective heat transfer to the fluid on the right wall increases as Bi increases. The presence of internal heat generation will contribute to more temperature on the right side of the wall. Meanwhile, the effects of Bi_H are illustrated in Figures 9. Based on Figure 9a, backflow only occurs with $Bi_H = 6$ and the maximum velocity occurs at the hotter wall. Figure 9b shows the temperature profiles are more prominent at the colder wall. The temperature then approached the value of 0.4 at the hot border.

(a)
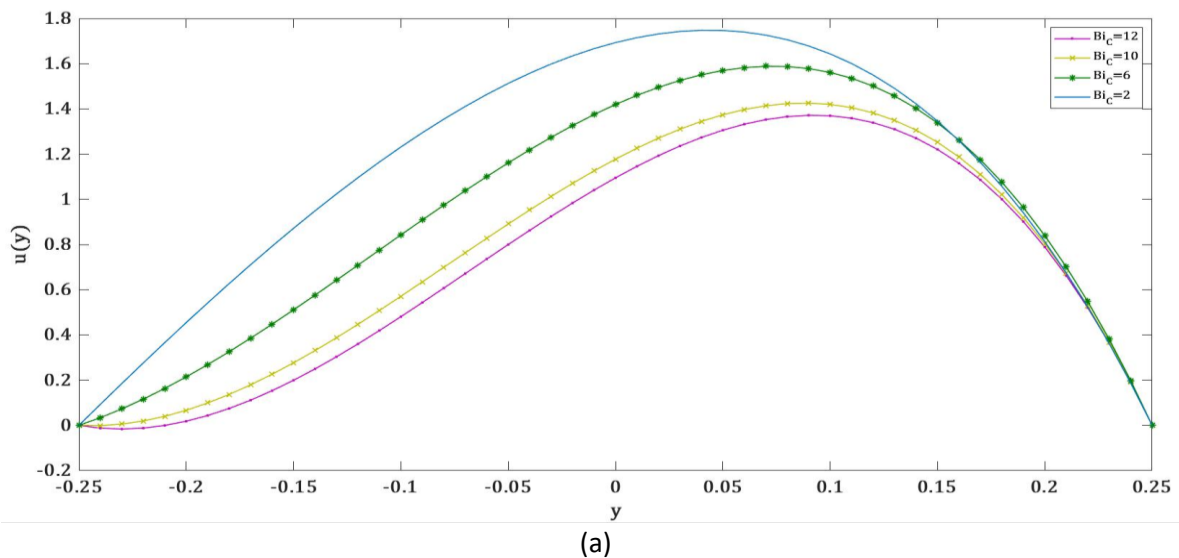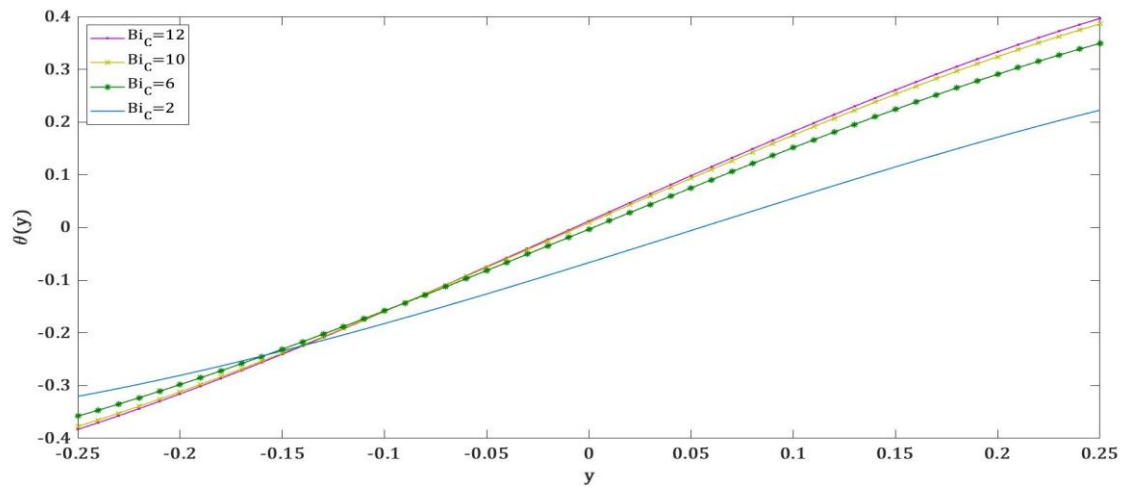
(b)

Fig. 8. Velocity and temperature profiles of non-Darcy flow for different values of Bi_C with $Bi_H = 10, GR = 120, Br = 0.002, Da = 2, F = 3, G = 10$ and $\lambda = 1$
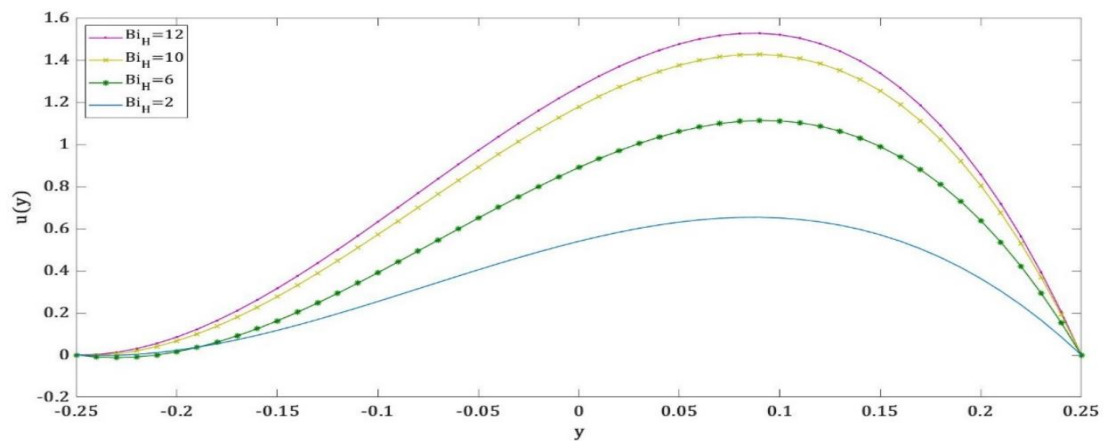
(a)
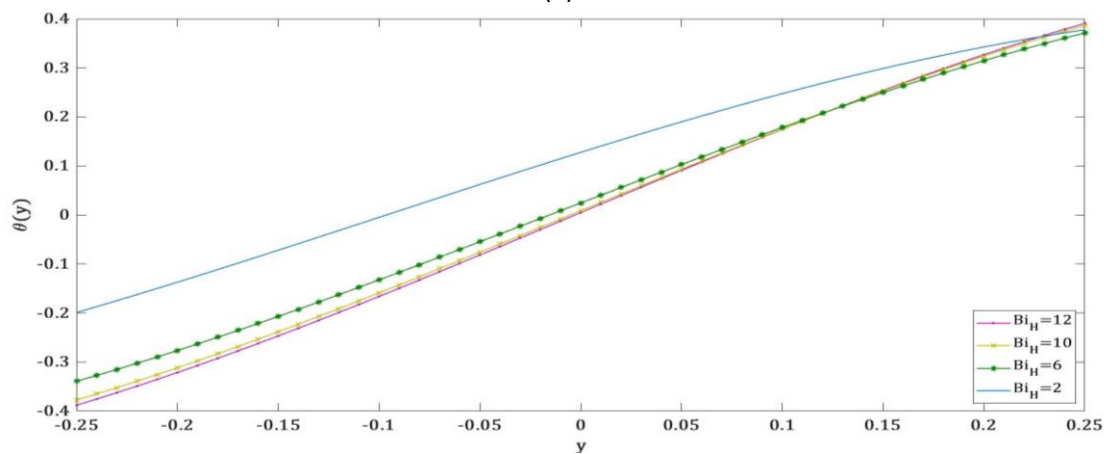
(b)

Fig. 9. Velocity and temperature profiles of non-Darcy flow for different values of Bi_H with $Bi_C = 10, GR = 120, Br = 0.002, Da = 2, F = 3, G = 10$ and $\lambda = 1$

Figures 10 depict the effect of three boundary conditions on temperature on velocity and temperature profiles. The Neumann boundary condition is met when $Bi = 0$. The hot side of the channel is completely insulated, and there is no convective heat transfer to the cold wall. Thus, both

the velocity and temperature profiles remain constant. Meanwhile, when $Bi = 10$, it relates to the Robin boundary condition and the Dirichlet boundary condition employed in $Bi = \infty$. When Bi increases, the channel thermal resistance at the cool wall falls while the temperature profiles at the hot wall increase. As the peak velocity and velocities in the peak area increased toward the hotter wall, this phenomenon occurred. This phenomenon occurred as the peak velocity and velocities in the peak area increased toward the hotter wall. This impact was produced by increased buoyant forces induced by the increased intensity of the convective process on the channel. As a result, the higher value of Bi in the Dirichlet boundary condition, the greater the amplitude of the velocity and temperature profile at the right wall of the channel.

This study should be considered important physical properties to maximize the heat transfer efficiency with the existence of internal heat generation. The Nusselt number, Nu, represents the heat transfer rate. Nu_C refers to the colder wall and Nu_H refers to the warmer wall. Figure 11 indicates the variation of Nu_C and Nu_H as a function of GR. As GR grows, the action of buoyant force works on the flow to raise fluid velocity with Robin and Dirichlet boundary conditions. Hence, this situation enhances the convection heat transfer and increases the Nusselt number. Nu_H decreases when GR rises, with the most extreme changes occurring in the Dirichlet condition. Furthermore, Figures 12 show the effect of Br on values of Nu_C and Nu_H, respectively. The heat transfer curve can be seen as more value of Br is applied for the Robin and becomes more linear for the Dirichlet boundary condition.

(a)

(b)
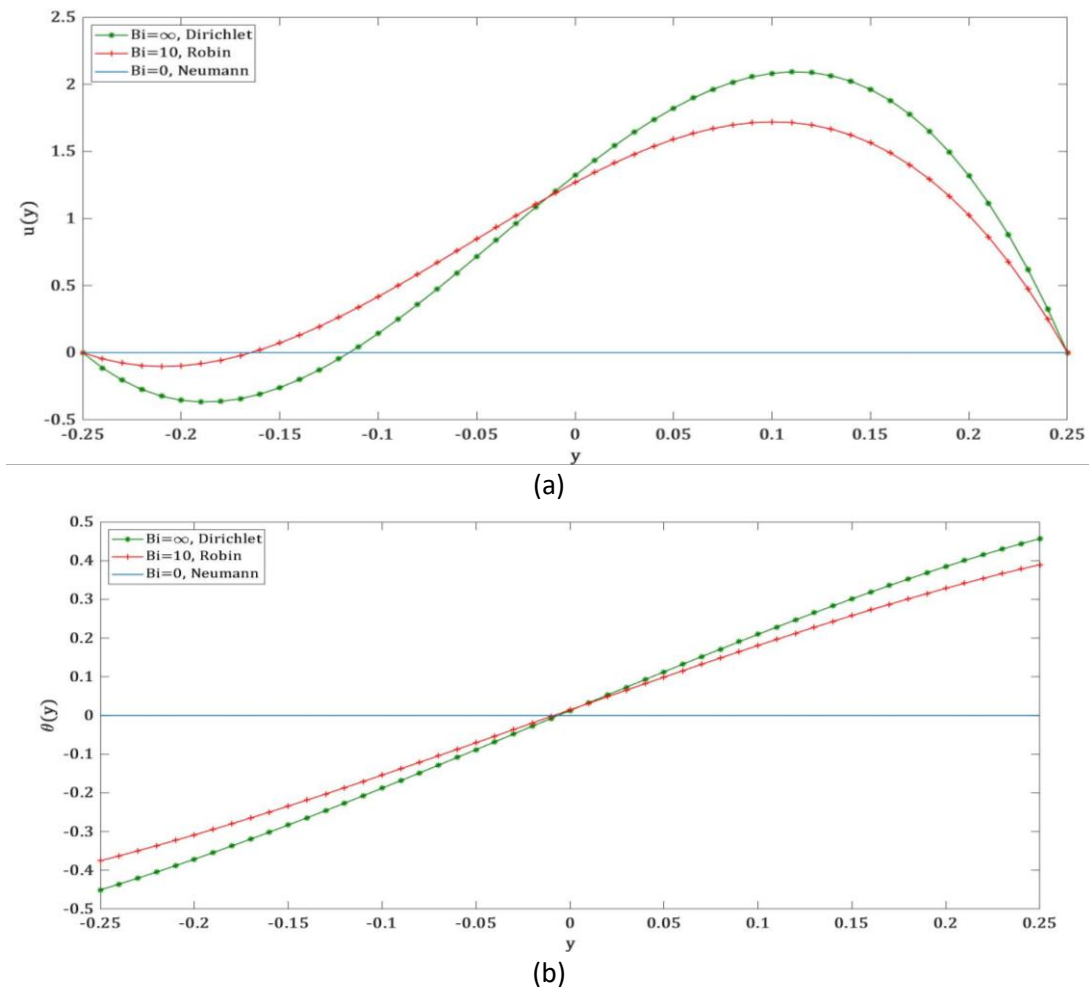
Fig. 10. The Influence of Three Kinds of Boundary Conditions on (a)velocity and (b) temperature profiles with $GR = 120, Br = 0.002, Da = 2, F = 3, G = 10$ and $\lambda = 1$
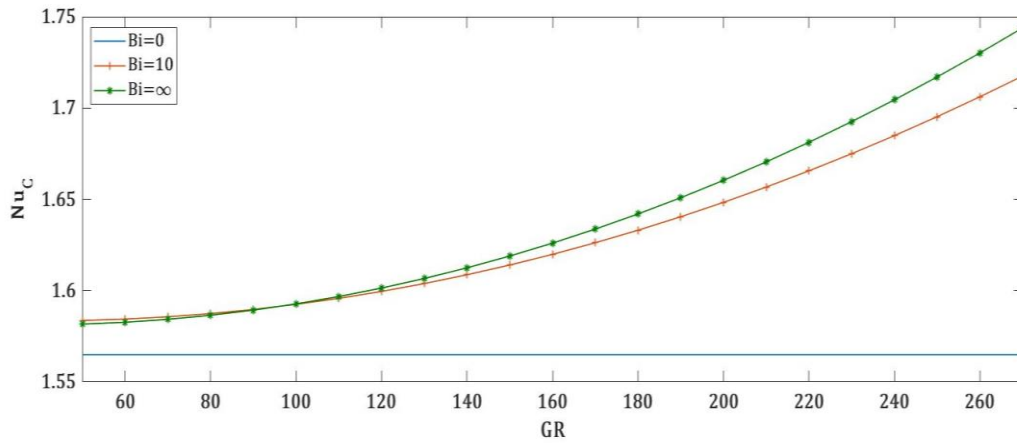
(a)
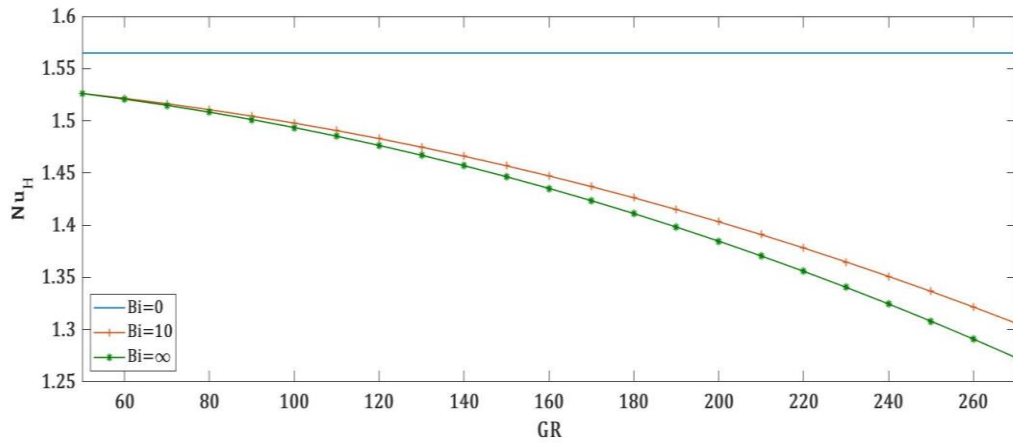
(b)

Fig. 11. The effect of GR on Nu_C and Nu_H for three kinds of boundary conditions on temperature where $Bi = Bi_C = Bi_H$, $Br = 0.002$, $Da = 2$, $F = 3$, $G = 10$ and $\lambda = 1$
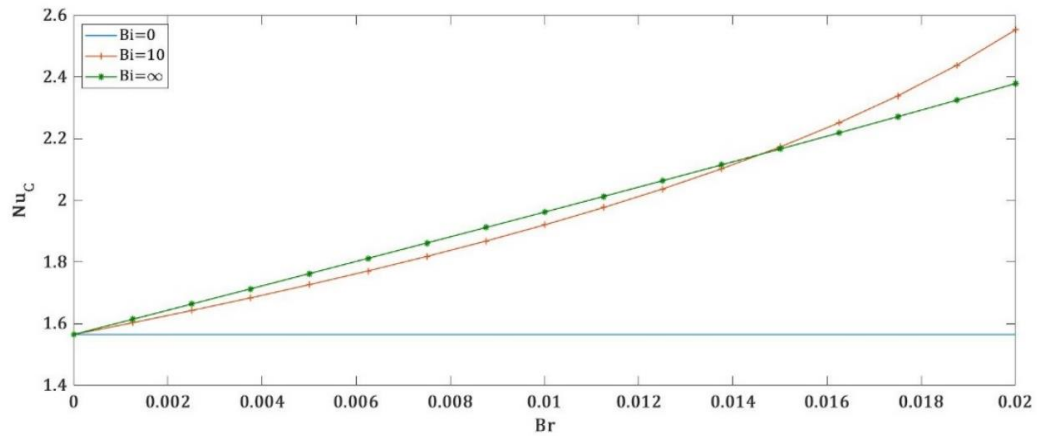
(a)
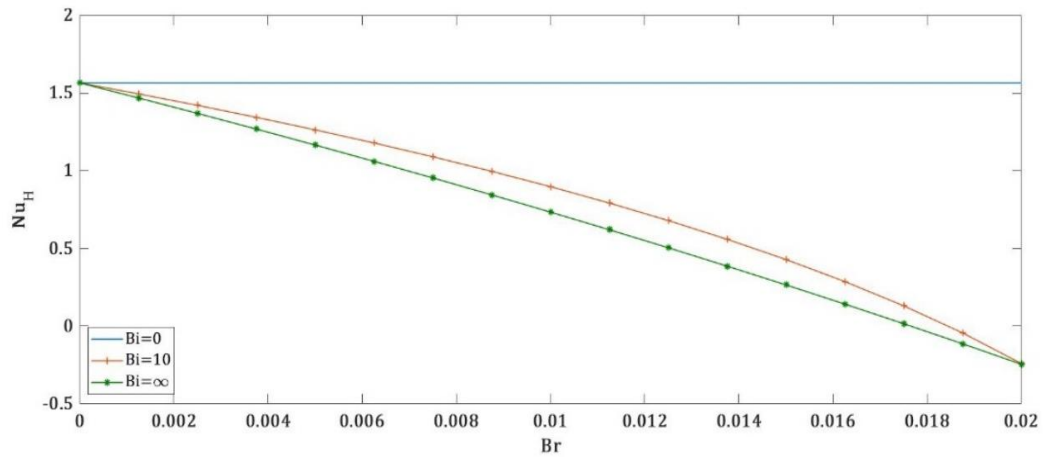
(b)

Fig. 12. The effect of Brinkman number, Br on Nu_C and Nu_H for three kinds of boundary conditions on temperature where $Bi = Bi_C = Bi_H$, $GR = 180$, $Da = 2$, $F = 3$, $G = 10$ and $\lambda = 1$
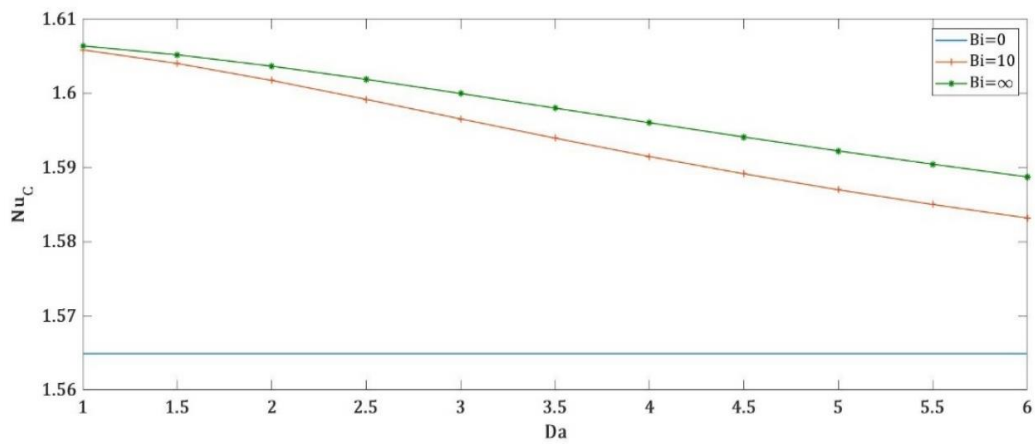
(a)
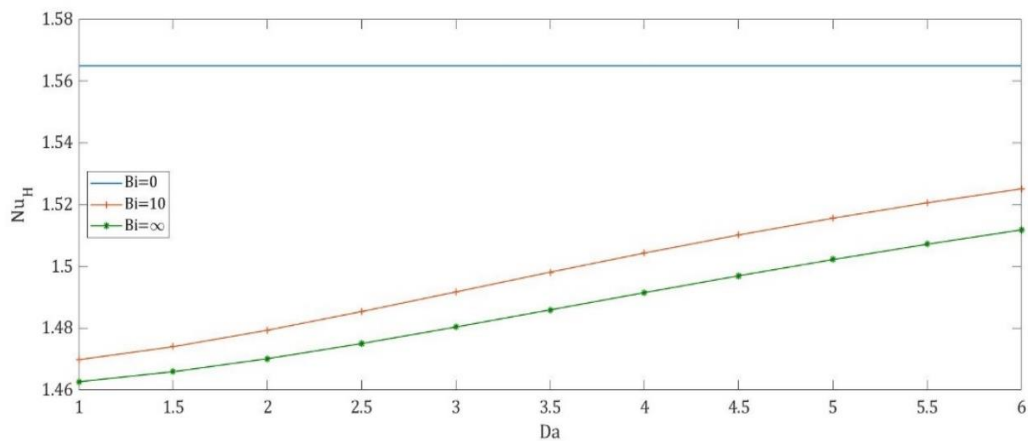
(b)

Fig. 13. The effect of Da on Nu_C and Nu_H for three kinds of boundary conditions on temperature where $Bi = Bi_C = Bi_H$, $GR = 120$, $Br = 0.002$, $F = 3$, $G = 10$ and $\lambda = 1$

The effects of Da on Nu_C and Nu_H for three kinds of boundary conditions are graphically presented in Figures 13a and 13b, respectively. When applying the Robin boundary condition, Nu_H

increases for the Robin boundary condition and becomes a constant rate as the Dirichlet boundary condition with the increasing number of Da is applied. These circumstances occurred because a high Da number results in a high permeability. Thus, the fluid experiences a relatively minor resistance as the fluid flows, leading to higher speed and increasing heat transfer rates. Besides, the effects of F on Nu_C and Nu_H are shown in Figure 14. The resulting graphs are nearly flat with an increase in F, demonstrating that the influence of F on both Nusselt values is modest compared to other factors. Considering that F has such a small impact on both Nusselt numbers, it is agreed that F has no bearing on the Nusselt numbers at all. Figures 11-14 show that G, Br, Da and F does not substantially affect Nusselt number values for the Neumann boundary condition. When $Bi = 0$, the hot side of the channel is completely insulated and no convective heat transfer to the cold wall occurs. Hence, both heat transfer profiles are constant.

The consequences of internal heat generation, G, on the two Nusselt numbers are shown in Figure 15. We can see that the profiles based on G do not remain constant as what happened on other parameters on the Neumann boundary condition. Inconsistent heat transmission rates can be attributed to the internal heat generated. As G increased, the heat transmission speed of Robin was higher than the Dirichlet boundary condition on the cool wall and at a lesser rate on the hotter wall. The Dirichlet boundary condition has linear profiles for both heat transfer rates. Furthermore, the effects of λ on Nu are displayed in Figures 16. Both graphs show that starting with a low value of λ, the Nusselt number dramatically increases when larger values of λ are used. When $\lambda =2$, Figure 16a portrays it reaching the highest heat transfer rate at the cool wall and drops after that because of the odd exponent number applied, which makes it decline. Both Nu profiles portray the constant rate as more value of λ is applied. This constant rate of heat transfer happened because G has a greater impact on heat transfer than the effects of the local heating exponent λ on heat transfer.
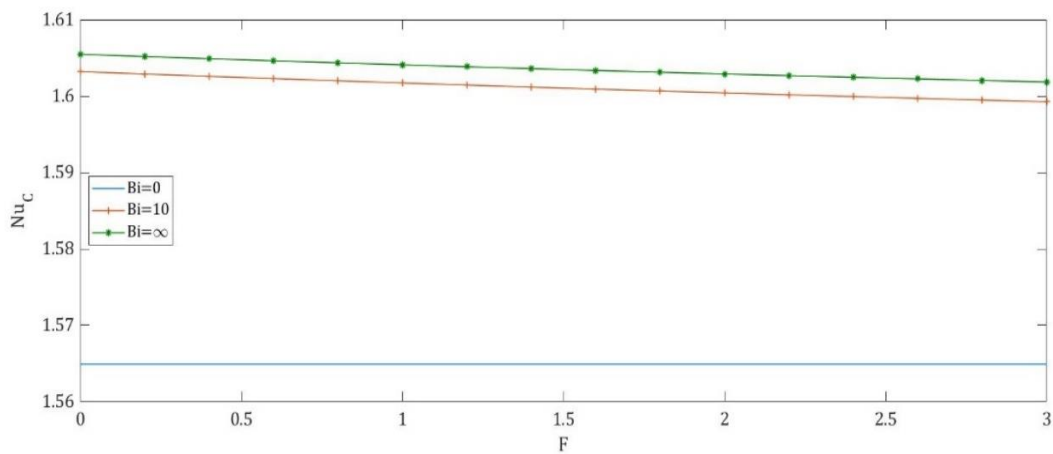
(a)
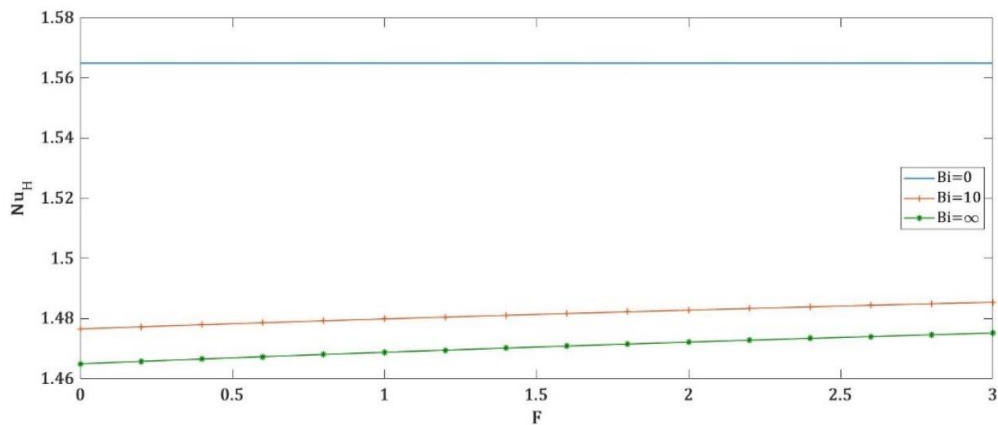
(b)

Fig. 14. The effect of F on Nu_C and Nu_H for three kinds of boundary conditions on temperature where $Bi = Bi_C = Bi_H$, $GR = 120$, $Br = 0.002$, $Da = 2$, $G = 10$ and $\lambda = 1$
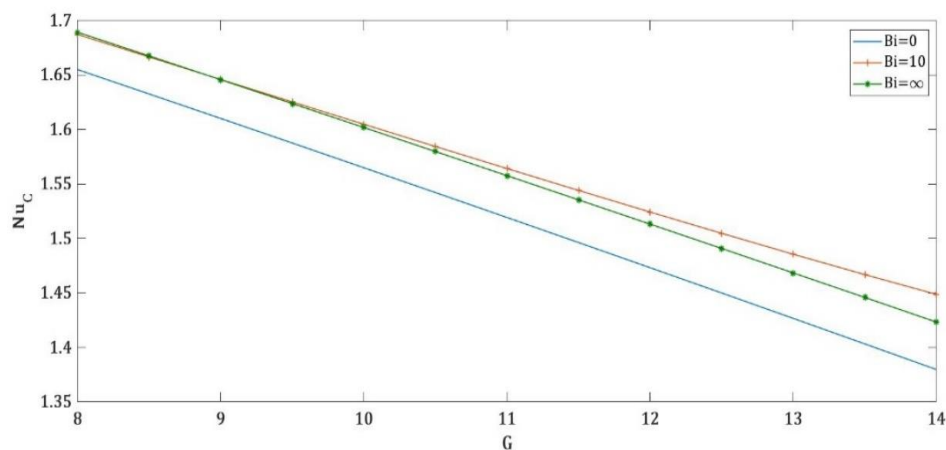
(a)
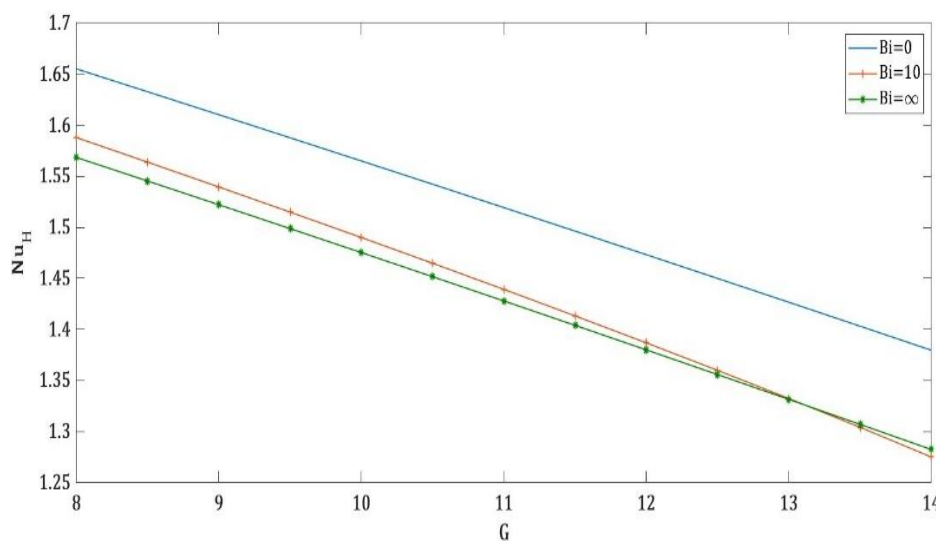
(b)

Fig. 15. The effect of G on Nu_C and Nu_H for three kinds of boundary conditions on temperature where $Bi = Bi_C = Bi_H$, $GR = 120$, $Br = 0.002$, $Da = 2$, $F = 3$ and $\lambda = 1$

(a)

(b)
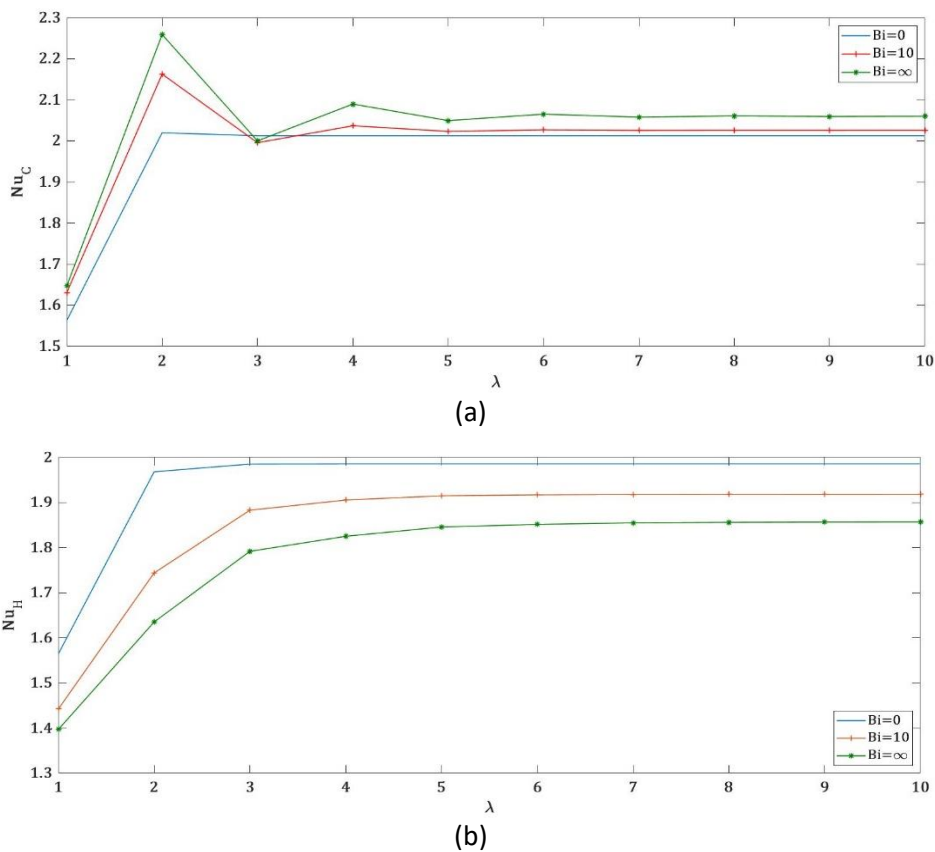
Fig. 16. The effect of λ on Nu_C and Nu_H for three kinds of boundary conditions on temperature where $Bi = Bi_C = Bi_H$, $GR = 180$, $Br = 0.002$, $Da = 2$, $F = 3$ and $G = 10$

4. Conclusions

The flow and heat transfer within a fully-developed non-Darcy flow via a vertical channel were investigated in this study using the three kinds of boundary conditions on temperature. In this research, the influence of various factors on velocity and temperature profiles and the local Nusselt number was graphically observed. The following are the key findings:

i. Raising the mixed convection parameter makes the velocity distribution less uniform.
ii. Flow reversal severity increases under Robin and Dirichlet conditions by enhancing Darcy and Forchheimer numbers and reducing Brinkman and internal heat generation values.
iii. The rise in Brinkman numbers enhances the temperature profiles. Nusselt number at both walls for all cases for the Neumann boundary condition remains constant except for internal heat generation and local heating exponent parameters.
iv. Nusselt numbers at both walls remain constant for the Neumann boundary condition when all parameters except internal heat production and local heat exponent are changed.
v. For sufficiently large mixed convection parameters, the Robin boundary condition looks preferable to the Neumann boundary condition, while the Dirichlet boundary condition appears impractical.

Acknowledgement

References

[1] Agrawal, H. C. "A variational method for combined free and forced convection in channels." *International Journal of Heat and Mass Transfer* 5, no. 6 (1962): 439-444. https://doi.org/10.1016/0017-9310(62)90155-2

[2] Barletta, Antonio. "Laminar mixed convection with viscous dissipation in a vertical channel." *International Journal of Heat and Mass Transfer* 41, no. 22 (1998): 3501-3513. https://doi.org/10.1016/S0017-9310(98)00074-X

[3] Bayareh, Morteza, Azam Usefian, and Afshin Ahmadi Nadooshan. "Rapid mixing of Newtonian and non-Newtonian fluids in a three-dimensional micro-mixer using non-uniform magnetic field." *Journal of Heat and Mass Transfer Research* 6, no. 1 (2019): 55-61.

[4] Broniarz-Press, Lubomira, and Karol Pralat. "Thermal conductivity of Newtonian and non-Newtonian liquids." *International journal of heat and mass transfer* 52, no. 21-22 (2009): 4701-4710. https://doi.org/10.1016/j.ijheatmasstransfer.2009.06.019

[5] Chinyoka, T. "Computational dynamics of a thermally decomposable viscoelastic lubricant under shear." (2008): 121201. https://doi.org/10.1115/1.2978993

[6] Ferdows, M., M. G. Murtaza, and M. D. Shamshuddin. "Effect of internal heat generation on free convective power-law variable temperature past a vertical plate considering exponential variable viscosity and thermal conductivity." *Journal of the Egyptian Mathematical Society* 27 (2019): 1-11. https://doi.org/10.1186/s42787-019-0062-5

[7] Kalaitzis, A., M. Makrygianni, I. Theodorakos, A. Hatziapostolou, S. Melamed, A. Kabla, F. de la Vega, and I. Zergioti. "Jetting dynamics of Newtonian and non-Newtonian fluids via laser-induced forward transfer: Experimental and simulation studies." *Applied Surface Science* 465 (2019): 136-142. https://doi.org/10.1016/j.apsusc.2018.09.084

[8] Kalyan, Shreedevi, and Ashwini Sharan. "Effect of material parameter on mixed convective fully developed micropolar fluid flow in a vertical channel." *Heat Transfer* 50, no. 6 (2021): 5853-5864. https://doi.org/10.1002/htj.22152

[9] Kanareykin, Aleksandr Ivanovich. "Energy calculation of the temperature field of an elliptical body without internal heat sources under boundary conditions of the third kind." In *IOP Conference Series: Earth and Environmental Science*, vol. 1045, no. 1, p. 012068. IOP Publishing, 2022. https://doi.org/10.1088/1755-1315/1045/1/012068

[10] Kumar, J. Prathap, Jawali C. Umavathi, Ali J. Chamkha, and Y. Ramarao. "Mixed convective heat transfer of immiscible fluids in a vertical channel with boundary conditions of the third kind." *Computational Thermal Sciences: An International Journal* 9, no. 5 (2017). https://doi.org/10.1615/ComputThermalScien.2017019221

[11] Mealey, L. R., and J. H. Merkin. "Steady finite Rayleigh number convective flows in a porous medium with internal heat generation." *International Journal of Thermal Sciences* 48, no. 6 (2009): 1068-1080. https://doi.org/10.1016/j.ijthermalsci.2008.10.008

[12] Makhatar, Nur Asiah Mohd, P. G. Siddheshwar, Habibis Saleh, and Ishak Hashim. "Oberbeck–Boussinesq free convection of water based nanoliquids in a vertical channel using Dirichlet, Neumann and Robin boundary conditions on temperature." *Alexandria Engineering Journal* 55, no. 3 (2016): 2285-2297. https://doi.org/10.1016/j.aej.2016.05.010

[13] Pazera, Ewelina. "Heat Transfer in Periodically Laminated Structures–Third Type Boundary Conditions." *International Journal of Computational Methods* 18, no. 03 (2021): 2041011. . https://doi.org/10.1142/S021987622041011X

[14] Prasad, Kerehalli Vinayaka, P. Mallikarjun, and Hanumesh Vaidya. "Mixed convective fully developed flow in a vertical channel in the presence of thermal radiation and viscous dissipation." (2017). https://doi.org/10.1515/ijame-2017-0008

[15] Saba, Fitnat, Naveed Ahmed, Saqib Hussain, Umar Khan, Syed Tauseef Mohyud-Din, and Maslina Darus. "Thermal analysis of nanofluid flow over a curved stretching surface suspended by carbon nanotubes with internal heat generation." *Applied Sciences* 8, no. 3 (2018): 395. https://doi.org/10.3390/app8030395

[16] Saleh, Habibis, Ishak Hashim, and Sri Basriati. "Flow reversal of fully developed mixed convection in a vertical channel with chemical reaction." *International Journal of Chemical Engineering* 2013 (2013). https://doi.org/10.1155/2013/310273

[17] Scheidegger, Adrian E. *The physics of flow through porous media*. University of Toronto press, 1957. https://doi.org/10.3138/9781487583750

[18] Tao, L. N. 1960. "On Combined Free and Forced Convection in Channels". *Journal Of Heat Transfer* 82 (3): 233-238. https://doi.org/10.1115/1.3679915

[19] Travis, Bryan, and Peter Olson. "Convection with internal heat sources and thermal turbulence in the Earth's mantle." *Geophysical Journal International* 118, no. 1 (1994): 1-19. https://doi.org/10.1111/j.1365-246X.1994.tb04671.x

[20] Tritton, D. J., and M. N. Zarraga. "Convection in horizontal layers with internal heat generation. Experiments." *Journal of Fluid Mechanics* 30, no. 1 (1967): 21-31. https://doi.org/10.1017/S0022112067001272

[21] Umavathi, Jawali C., Mikhail A. Sheremet, Bernardo Buonomo, and Oronzio Manca. "Convection in a vertical duct under the chemical reaction influence using Robin boundary conditions." *Thermal Science and Engineering Progress* 15 (2020): 100440. https://doi.org/10.1016/j.tsep.2019.100440

[22] Wu, Yu-Shu. *Theoretical studies on non-Newtonian and Newtonian fluid flow through porous media*. University of California, Berkeley, 1990. https://doi.org/10.2172/7189244

[23] Zanchini, Enzo. "Effect of viscous dissipation on mixed convection in a vertical channel with boundary conditions of the third kind." *International Journal of Heat and Mass Transfer* 41, no. 23 (1998): 3949-3959. https://doi.org/10.1016/S0017-9310(98)00114-8

[24] Jahan, Sultana, M. Ferdows, Md Shamshuddin, and Khairy Zaimi. "Radiative mixed convection flow over a moving needle saturated with non-isothermal hybrid nanofluid." *Journal of Advanced Research in Fluid Mechanics and Thermal Sciences* 88, no. 1 (2021): 81-93. https://doi.org/10.37934/arfmts.88.1.8193

[25] Bakar, Norhaliza Abu, and Rozaini Roslan. "Mixed convection in a lid-driven horizontal cavity in the presence of internal heat generation or absorption." *Journal of Advanced Research in Numerical Heat Transfer* 3, no. 1 (2020): 1-11.